Published in final edited form as:
Biosens Bioelectron. 2015 February 15; 64: 138–146. doi:10.1016/j.bios.2014.08.072.

A comparative study of different protein immobilization methods for the construction of an efficient nano-structured lactate oxidase-SWCNT-biosensor

Miraida Pagán, **Dámaris Suazo**, **Nicole del Toro**, and **Kai Griebenow***
Department of Chemistry, University of Puerto Rico, Río Piedras Campus, P.O. Box 23346, San Juan, Puerto Rico 00931-3346

Abstract

We constructed lactate biosensors by immobilization of lactate oxidase (LOx) onto a single-walled carbon nanotube (SWCNT) electrode. The first step of the sensor construction was the immobilization of oxidized SWCNT onto a platinum electrode modified with 4-aminothiophenol (4-ATP). Two enzyme immobilization methods were used to construct the biosensors, i.e., covalent immobilization using 1-ethyl-3-(3-dimethylaminopropyl) carbodiimide hydrochloride (EDC) and physical adsorption. Atomic force microscopy (AFM) experiments confirmed the immobilization of SWCNT during the biosensor construction and X-ray photoelectron spectroscopy (XPS) experiments confirmed covalent immobilization of LOx onto the SWCNT in the first method. The biosensor based on covalent enzyme immobilization showed a sensitivity of 5.8 μA/mM, a linearity up to 0.12 mM of L-lactate, and a detection limit of 4.0 μM. The biosensor based on protein adsorption displayed a sensitivity of 9.4 μA/mM, retaining linearity up to 0.18 mM of L-lactate with a detection limit of 3.0 μM. The difference in the biosensor response can be attributed to protein conformational or dynamical changes during covalent immobilization. The stability of the biosensors was tested at different temperatures and after different storage periods. The thermostability of the biosensors after incubation at 60°C demonstrated that the biosensor with covalently immobilized LOx retained a higher response compare with the adsorbed protein. Long-term stability experiments show a better residual activity of 40% for the covalently immobilized protein compared to 20% of residual activity for the adsorbed protein after 25 d storage. Covalent protein immobilization was superior compared to adsorption in preserving biosensor functionality over extended time period.

Keywords

covalent immobilization; lactate biosensor; lactate oxidase; physical adsorption; protein immobilization; protein stability

miraida.pagan@gmail.com. damysuazo@gmail.com. nicolitapg@gmail.com. *Corresponding author: Telephone: (787) 764-0000 x. 7374, Fax: (787) 756-8284, kai.griebenow@gmail.com, Address: P.O. Box 23346, San Juan, Puerto Rico 00931-3346.

1. Introduction

Precise measurement of the serum lactate concentration is essential for the diagnosis and medical management of various diseases. The normal range of lactate in blood is 0.5-2.5 mM (Cowan et al. 1984). An elevated blood lactate concentration can indicate multiple organ failure or septic shock and can be used as a sensitive indicator of survival during surgical operations or intensive care therapy (Bakker et al. 1996; Shapiro et al. 2005). Measurement of blood lactate is also relevant in the sport medicine, particularly for estimation of the physiological condition of athletes. Sensors developed to measure lactate frequently employ lactate oxidase (LOx), the model enzyme chosen by us in this work. This protein belongs to the family of flavin mononucleotide-dependent oxidizing enzymes that catalyzes the oxidation of L-lactate to pyruvate. This reaction produces as by-product hydrogen peroxide (H_2O_2) (Furuichi et al. 2008), which can be detected using an electrochemical sensor (for details see Fig. S1 in the Supplementary Materials).

Nanomaterials represent an excellent tool for coupling of biomolecules with electronic circuits, e.g., by using single-walled carbon-nanotubes (SWCNT). Studies on the behavior of biomolecules attached to carbon-based nano-materials have received increased attention in the past decade (Vashist et al. 2011). Such nano-materials possess unique physical and chemical properties (e.g., excellent electronic, thermal, and mechanical properties) that enable small currents to be detected and thus allow the detection of target molecules at extremely low levels. Another advantage of using carbon nano-materials is that they can be oxidized and functionalized allowing for the use of different immobilization methods. The alignment of SWCNT on electrodes produces faster charge transfer rates compared to randomly dispersed SWCNT and maximizes the number of SWCNT ends exposed at the electrode surface making them superior for the attachment of biomolecules (Flavel et al. 2010). Vertically aligned SWCNT can be used to study basic concepts of biomolecules on sensors, but can also be applied to more complex systems, such as, nanoelectrode devices with patterned vertically align single-walled carbon nanofibers (Gupta et al. 2014). We therefore aimed at developing a biosensor utilizing aligned SWCNT.

Enzyme immobilization is one of the key steps that can be addressed to improve the biosensor response, thermostability, and long-term stability. Covalent immobilization of the protein provides a more durable attachment and avoids the loss of protein via leaching when it is in contact with the solvent during analysis thus enhancing the long-term stability of the sensor (Kim et al. 2006). Adsorption on the other hand provides a simple way to immobilize a variety of proteins on CNTs. However, one major concern is the long-term stability of the biosensor since the immobilized protein is exposed to the solvent and therefore can be lost gradually during use.

Different papers report on the immobilization of LOx onto CNTs by adsorption (e.g., sol-gel) (Huang et al. 2008; Goran et al. 2011; Haghighi and Bozorgzadeh 2011; Taurino et al. 2013), by covalent immobilization with glutaraldehyde (Yamamoto et al. 2003), or by using the popular cross-linker EDC (Wang et al. 2012). Despite the fact that LOx has been covalently immobilized frequently onto carbon nanomaterials, there is still a lack of detailed studies investigating the structural, functional, and stability consequences of this. Herein, we

constructed two lactate biosensors by physically adsorbing and by covalently immobilizing LOx onto vertically aligned SWCNT (**Fig. 1**). We used SWCNT in this paper solely because they are a step in the development of a lab-on-a-chip devise in a collaboration of our group with NASA. It is entirely possible that other substrates (e.g., graphene, multi walled-CNT) that offer more surface area and immobilization sites (e.g., carboxyl groups) are even more suitable. Comparative studies of the catalytic performance of both biosensors were done. AFM and XPS were used to study in detail the immobilization of the protein onto the sensor. The stability of the biosensors was tested by temperature shift experiments and by long-term storage experiments.

This paper reports, for the first time, an XPS study of the EDC carbodiimide reaction using sulfo-NHS to verify the covalent immobilization of LOx onto SWCNT. The sulfite group of the intermediate in this reaction has not previously been studied by XPS. In addition, we were able to demonstrate that the used of covalent immobilization to construct the biosensor results in superior long-term stability compared with the adsorbed LOx biosensor and LOx biosensors described in the literature (Weber et al. 2006; Taurino et al. 2013).

2. MATERIALS AND METHODS

2.1. Reagents and Substrates

Lactate oxidase was obtained from Wako Chemicals, USA (Richmond, VA). SWCNT with a diameter distribution of 0.8-1.2 nm and a length distribution of 100-1000 nm were purchased from Unidym Inc. (Houston, TX). Sulfo-N-hydroxysuccinimidyl (Sulfo-NHS) was purchased from Proteo Chem (Denver, CO). Sulfuric acid (optima grade) and alumina powders of 1.0, 0.3, and 0.05 μm diameter were obtained from Fisher Scientific (Fairlawn, NJ). *N*,*N'*-dicyclohexylcarbodiimide 99% (DCC), *N*,*N*-dimethylformamide (DMF), L-lactic acid, hydrogen peroxide 30 %, 4-aminothiophenol, KH_2PO_4, K_2HPO_4, $K_3Fe(CN)_6$, $K_4Fe(CN)_6$, 2-(N-morpholino)ethanesulfonic acid (MES) and 1-ethyl-3-(3-dimethylaminopropyl)carbodiimide hydrochloride were obtained from Sigma-Aldrich (Saint Louis, MO) and used as received.

2.2. Electrochemical Instrumentation

Cyclic voltammetry (CV) and chonoamperometry (CA) were performed using a PARSTAT 2273 electrochemical system (AMETEK Inc., Oak Ridge, TN) and a conventional three-electrode cell. Polycrystalline platinum (Pt) working electrodes (1.6 mm diameter), Ag/AgCl reference electrodes (Bio-analytical Systems Inc., West Lafayette, IN) and a Pt mesh counter electrode (Sigma-Aldrich) were used for electrochemical measurements. Quartz crystal microbalance polycrystalline Pt sensors from Inficon-Maxtek, Inc. (East Syracuse, NY) were used for XPS and AFM experiments.

2.3. Electrode Preparation

All polycrystalline Pt electrodes were mechanically polished using 1.0, 0.3, and 0.05 μm alumina powder and sonicated in nanopure water to eliminate alumina residues. Electrochemical polishing was performed by CV in a potential range from −0.20 V to 1.2 V

in 0.1 M H_2SO_4 at a 100 mV/sec scan rate until a reproducible voltammogram was observed.

Oxidation of SWCNT was done prior to the biosensor assembling by mixing concentrated HNO_3/H_2SO_4 (20 ml, 1:3 volume ratio) with the SWCNT followed by 10 h of sonication in a sonication bath at 40°C. The solid was filtered and washed with copious amount of distilled water until a neutral pH was reached and subsequently dried under vacuum (Rosario-Castro et al. 2010). The cleaned polycrystalline Pt electrodes were immersed in 4-ATP (1.0 M) ethanolic solution for 24 h to produce a self-assembly monolayer (SAM). Next, oxidized SWCNT were attached to the 4-ATP SAM by DCC conjugation (Nan et al. 2002). SWCNT were sonication in DMF (0.2 mg in 1 ml) and DCC added (2.4 mM). Later, the 4-ATP/Pt electrodes where immersed in the SWCNT suspension and incubated at 60°C in a water bath. After 12 h of immobilization, the electrode was gently washed with EtOH. In order to covalently attach the protein to the electrode, the SWCNTs were conjugated with the linker EDC (2.5 mM) and sulfo-NHS (4.5 mM) in 0.1 M MES buffer (pH 6.5). Subsequently, the electrode was gently washed with MES buffer and a drop of the protein solution (0.3 mM) in 0.1 M potassium phosphate buffer (PBS) pH 7.0 was placed onto the electrode and allowed to react for 24 h at 4°C. Each electrode was rinsed with buffer prior to use. A similar biosensor was constructed by physically adsorbing the protein onto the SWCNT-sensor.

2.4. Atomic Force Microscopy and X-Ray Photoelectron Spectroscopy Analysis

A Nanoscope IIIa-Multimode atomic force microscope from Digital Instruments, with a scanning probe microscope controller equipped with a He-Ne laser (638.2 nm) and a type E scanner was used for the AFM analysis. All samples were analyzed in tapping mode using a phosphorous doped Si cantilever from Veeco Instrument Inc. (Santa Clara, CA). XPS data was obtained using a PHI 5600ci spectrometer with an Al Kα X-ray source at 15 kV and 350 W. The pass energy used was 187.85 eV for the survey analysis and 58.7 eV for the high energy resolution studies.

2.5. Chronoamperometry Measurement

To determine the capability of the SWCNT sensor to detect H_2O_2, chronoamperometry measurements were performed in a cell holding 5.0 ml of PBS at pH 7.0. The biosensor was equilibrated for the first 300 s under constant stirring (300 rpm) and then consecutive additions of H_2O_2 (0.5 mM) were performed at 0.6 V. To determine the LOx biosensor response, similar chronoamperometry measurements were performed with consecutive additions of L-lactate (6.0 mM) at 0.6 V.

2.6. Biosensor Stability

2.6.1. Effect of Temperature on the Biosensor—To assess the effect of temperature on the biosensor response, each electrode was incubated at different temperatures from 15°C to 65°C for 15 min. Chronoamperometry experiments were done at each temperature using 6.0 mM of L-lactate at 0.6 V. A control experiment was done with LOx in solution, not immobilized onto the SWCNT electrode (0.67 μM LOx).

2.6.2. Thermostability of the Biosensors—Each biosensor was incubated at 60°C for 0 to 35 min. The current density of the biosensor was measured after each incubation time using 0.18 mM of L-lactate at 0.6 V.

2.6.3 Repeatability and Long-term Stability of the Biosensors—The repeatability of the biosensor response was determined from consecutive tests of the current density using 0.18 mM of L-lactate at 0.6 V. The long-term stability was tested measuring the percent of relative activity of the biosensor after storage at different temperature (i.e., 4°C and 30°C).

3. Results and Discussion

3.1. Electrochemical Characterization of the SWCNT-Sensor and the LOx Biosensor

The first step of the LOx biosensor construction was to modify the clean Pt surface with 4-ATP forming a SAM followed by the covalent immobilization of SWCNT (**Fig. 1**). Next, the enzyme LOx was covalently immobilized onto the SWCNT using EDC linker chemistry. CV was used to characterize the electrochemical response after each immobilization step by detecting the electron transfer of the electroactive species $K_3Fe(CN)_6/K_4Fe(CN)_6$ in buffer solution. The voltammogram of the bare electrode shows the typical reversible behavior of the electroactive species (0.28 V and 0.22 V) **(Figure S1-A)**. After the 4-ATP immobilization, the redox peak of the active species barely disappeared due to the blocking effect of the SAM, suggesting that a densely packed monolayer was formed and did not allow the ions to reach the electrode surface (Rosario-Castro et al. 2006). The formation of a well-defined SAM allows for the covalent attachment of short aligned oxidized SWCNT (Nan et al. 2002). After SWCNT immobilization onto the electrode, an increase in the current was observed. This can be due to capacitance changes since the surface area of the electrode after SWCNT immobilization increased relative to the 4-ATP SAM electrode area (Rosario-Castro et al. 2010). A slight decrease in the current was observed after LOx immobilization since the protein is blocking the SWCNT surface. The experimental data are consistent with the proposed biosensor assembly (**Fig. 1**).

Previous to the immobilization, the SWCNT were exposed to a strong oxidative treatment in order to reduce their length, activate their surface with carboxylic acid groups (-COOH), and covalently immobilize LOx. The redox behavior of the SWCNT carboxylic acid groups was monitored by CV in 0.5 M H_2SO_4 (**Fig. S1-B**). The presence of two redox peaks (0.45 and 0.47 V) suggests that the SAM-Pt electrode was modified with SWCNT and that those SWCNT were indeed activated with carboxylic groups (Wang et al. 2008).

In order to determine the efficiency of the SWCNT sensor to detect H_2O_2, chronoamperometry experiments were performed by consecutive addition of 0.5 mM H_2O_2 (**Fig. S2**). The same experiment was done with the bare Pt electrode without SWCNT. The SWCNT electrode presented a higher response than the bare electrode demonstrating that the use of SWCNT improved the detection of H_2O_2 (**Table S2**) as described in the literature (Saifuddin et al. 2013). CV experiments of the electrode with and without SWCNT in 2.0 mM H_2O_2 also demonstrate the superiority of the electrode with SWCNT over the bare Pt electrode (Fig. S2-C).

After protein immobilization onto the SWCNT sensor, it was necessary to characterize the biosensor by investigating the optimum potential that produce the highest current. The effect of applying different potentials (0.0-0.8 V) on the steady-state current produced by the lactate biosensor was also studied (**Figure S3-A)**. The steady-state current increased at increasing applied potential reaching a maximum at 0.6 V. The potential chosen for further amperometric experiments was 0.6 V. Moreover, different concentrations of LOx (10, 27 and 52 mg/ml) were covalently immobilized onto the SWCNT sensor to determine the optimum response of the sensor. The calibration curves (**Fig. S3-B**) of the different biosensors show a sensitivity of 2.31, 5.29, 3.72 μA/mM cm^2 at increasing LOx concentration. Further biosensor constructions were done using a LOx concentration of 27 mg/ml.

3.2. X-Ray Photoelectron Spectroscopy Experiments

XPS experiments were conducted to verify the chemistry of the covalent immobilization of LOx (**Fig. S4**). XPS experiments have been used previously to demonstrated the immobilization of different biomolecules onto sensors (e.g., glucose oxidase (Liu et al. 2004) and estrogen receptor (Im et al. 2010)). However, the data commonly reported in the literature show XPS spectra of the immobilized protein without presenting the data of the electrode previously activated with the linker (e.g. EDC/sulfo-NHS or glutaraldehyde). In most cases the authors simply assume that the covalent protein immobilization was achieved successfully. To provide evidence that demonstrate that the protein was actually covalently immobilized, we studied each step of the biosensor assembly and the covalent immobilization of the enzyme LOx onto the SWCNT-based biosensor by XPS. One paper in the literature reports the covalently immobilization of LOx onto a CNT-sensor using the linker EDC but no XPS or other experimental evidence directly support the covalent immobilization (Wang et al. 2012).

When sulfo-NHS and the EDC linker react with the carboxylic acid groups of the oxidized SWCNT they form a stable ester-sulfite intermediate group that can be monitored by XPS (**Figure 1**). **Figure 2** shows the high-resolution (HR) XPS spectra of S2p, C1s, N1s and O1s that describe each step of the biosensor construction. The spectra for the unmodified Pt electrode display small peaks in the C1s and O1s region. The emission peak for C1s results from environmental contamination, and the O1s peak results from any small amount of Pt oxide formed at the surface of the bare Pt electrode (Petrovykh et al. 2006). The spectra for the 4-ATP SAM on the Pt electrode show not only the same C1s and O1s peaks as the clean Pt electrode but also S2p, and N1s peaks. The sulfur (163.0 eV) and nitrogen (400.0 eV) peaks visible correspond to the 4-ATP SAM on the Pt electrode. The increase in the C1s peak (285.0 eV) is due to the presence of the carbon ring of 4-ATP. The third spectra show the immobilized SWCNT on the electrode. The presence of oxidized SWCNT is apparent by the increased intensity in the C1s and O1s peaks demonstrating the presence of carboxylic acid groups.

The spectra that correspond to SWCNT modified with the linker EDC and sulfo-NHS shows different peaks as the SWCNT spectra. The combination of the linker EDC and sulfo-NHS leads to an ester intermediate on the SWCNT. The ester intermediate has a sulfite group

(SO^{3-2}) that shows a binding energy at a higher value when compared to the sulfur group of 4-ATP (163.0 eV). Indeed, the spectrum shows the appearance of the Sp2 peak at a binding energy of 168.0 eV corresponding to the presence of the sulfite group. Another characteristic peak demonstrating the presence of the EDC ester intermediate is observed in the spectra of N1s. Two peaks are observed: one corresponding to the secondary amine and/or traces of the EDC imine at 400.0 eV and a second peak at 402.0 eV corresponding to the nitrogen-oxygen bond of the NHS ester. The higher binding energy of the second peak is due to the electronegativity of the oxygen (Im et al. 2010).

The last spectra correspond to the LOx immobilization onto the linker-modified SWCNT. Compatible with binding of the protein to the linker-CNT, the sulfite S2p peak of the linker vanishes. The disappearance of this peak is indicative of the formation of a covalent bond between the oxidized SWCNT and the protein. Additionally, an increase in the intensity of the peaks of C1s, N1s and O1s confirm the presence of the protein on the electrode. All observations are compatible with the idea of a covalently immobilized LOx on the surface of the oxidized SWCNT. The observations, nevertheless, cannot exclude that some LOx could also be bound to the SWCNT by adsorption.

3.3. Atomic Force Microscopy Studies

AFM in tapping mode was used to study the electrode surface morphology after each step of the biosensor assembly (**Fig. 3**). Image 3a and 3b represent the bare Pt electrode and the Pt electrode modified with a 4-ATP SAM, respectively. The images are very similar because of the short length of the 4-ATP SAM. A cross-section analysis reveals no significant change in Pt electrode surface height after 4-ATP immobilization (**Fig. 3f**).

Immobilization of the SWCNT, in contrast, leads to significant changes in the AFM image (**Fig. 3c**). The AFM image shows a surface height distribution of 73-142 nm. After subtracting the substrate height, the immobilized SWCNT are about 51-121 nm long with most of them around 51 nm in length. Previous research has demonstrated that the use of short-thiol-functionalized CNT (Liu et al. 2000; Nan et al. 2002) or immobilization of short CNT onto thiol SAM (e.g., 4-ATP, alkanethiol) (Sanchez-Pomales and Cabrera 2007; Rosario-Castro et al. 2010; Moore et al. 2011) will lead to the immobilization of perpendicularly aligned nanotubes on the surface leaving one of the CNT-ends available for further modification (e.g., protein immobilization). The use of a SAM with short SWCNT should favor the perpendicular alignment. It is therefore important to verify that the oxidation step reduces the lengths of the SWCNT. AFM images of adsorbed SWCNT before and after the oxidation step demonstrate that indeed the oxidation procedure shortened them (Fig. S6). Other research groups have reported similar results (Sanchez-Pomales and Cabrera 2007; Flavel et al. 2010; Rosario-Castro et al. 2010; Moore et al. 2011).

We verified the SWCNT alignment on the electrode by scanning electron microscopy (SEM) of a SWCNT/4-ATP modified Pt electrode (Fig. S5). It is apparent that mostly the SWCNT are visible as small dots or circles suggesting the perpendicular alignment of the SWCNT on the surface.

The AFM images obtained after physical adsorption of the protein and after covalent protein immobilization (**Fig. 3e, 3d and 3g**) show peaks with around ca. 82 nm of height. After subtracting the surface height of the SWCNT image (~73 nm) from the surface height after protein immobilization, the resulting height of ca. 8 nm corresponds to LOx. LOx is a protein composed of four sub-units, which measures ca. 4.6 nm - 9.7 nm (Boero et al. 2011). Thus, each data point obtained by AFM supports that the assembly of the biosensor followed the route suggested (**Fig. 1**).

3.4. Chronoamperometry and Calibration Curve of the LOx Biosensor

The protein immobilization step is a key event affecting the stability and the response of an enzyme-based sensor. Among the different protein immobilization methods (e.g., covalent coupling, physical adsorption, entrapment of the protein in a gel or polymer, and cross-linking between biomolecules (Sassolas et al. 2012)) the most used method for LOx immobilization is physical adsorption (**Table S1**). However, a drawback of physical adsorption of biomolecules is that they can desorb and leach during application when the enzyme gets in contact with the solution thus reducing the biosensor response and long-term stability (Cang-Rong and Pastorin 2009; Saifuddin et al. 2013). Covalent immobilization represents a superior alternative to adsorption and extends the life of the biosensor. However, for some proteins covalent immobilization can cause structural changes and function loss. Herein, the response of the LOx biosensor was examined using two different enzyme immobilization methods: physical adsorption and covalent coupling via carbodiimide chemistry.

The chronoamperometry experiment shows an increase in the current as response upon addition of L-lactate for both biosensors (**Fig. 4A**). The calibration curve of the biosensor with the physically adsorbed enzyme exhibits a linear response up to 0.18 ± 0.03 mM of lactate reaching saturation at a concentration of 0.90 mM (**Fig. 4B**). The sensitivity of this biosensor was determined to be 9.4 ± 0.6 μA/mM cm^2 with a detection limit of 3.0 ± 0.2 μM. The sensitivity of the biosensor with the covalently attached enzyme was determined to be 5.8 ± 0.6 μA/mM cm^2 with a detection limit of 4.0 ± 0.8 μM (**Table S3**).

We observe that physically adsorbed LOx had a higher sensitivity than the covalently immobilized protein. This result is in agreement with the covalent immobilization of different proteins on SWCNT (e.g. glucose oxidase (Stavyiannoudaki et al. 2009) and amyloglucosidase (Cang-Rong and Pastorin 2009)). The lower sensitivity for the covalent method can potentially be attributed to different factors. The formation of new bonds involving the amine groups of the protein lysine residues with the SWCNT can disrupt the structural integrity of the enzyme and therefore the activity of the enzyme. CD studies of the protein amyloglucosidase immobilized on CNT using EDC linker chemistry reveals protein structural changes after immobilization compared with the adsorbed enzyme (Cang-Rong and Pastorin 2009). Adsorption of the protein onto the CNTs in contrast involves hydrophobic and electrostatic interactions which might cause less structural distortion (Saifuddin et al. 2013). However, such formation of new bonds can affect the sensitivity of the biosensor because new bonds reduce the structural mobility of the enzyme. Reduced structural mobility has been linked to reduced enzyme activity for dissolved enzymes (Pagán

et al. 2009; Solá et al. 2007). Furthermore, it has been pointed out that covalent immobilization should affect protein dynamics more than simple adsorption (Hanefeld et al. 2009). Other possible reasons can include low enzyme loading since during covalent immobilization the enzyme reacts only with the carboxylic acid groups and not all the SWCNT surface (Cang-Rong and Pastorin 2009). Compared to previous research of LOx-CNT biosensors (**Table S1**), our biosensors show comparable sensitivity, linear range, and detection limit.

3.5 Effect of Temperature on LOx Biosensor Performance

The effect of the temperature on the biosensor was studied to determine the optimum working temperature and to get an idea on storage stability. Studies on different protein-CNT conjugates revealed that the protein activity was retained after immobilization and the thermostability of the conjugates increased relative to the enzyme in solution (Asuri et al. 2006). In order to investigate the effect of the temperature on the biosensor response, the two biosensors were incubated for 15 min at temperatures from 15°C to 65°C. After the incubation period, chronoamperometry experiments were used to determine the sensitivity of each biosensor (**Fig. 5A**).

The physically adsorbed LOx sensor showed a response increase at increasing temperature, reaching a maximum at 25°C followed by a gradual decrease. The biosensor with the covalently immobilized protein showed an increase in response up to a maximum temperature of 30°C. Comparing both biosensors it is evident that at higher temperatures (>30°C) the covalently immobilized protein showed a higher response throughout the whole temperature profile compared to the one with adsorbed protein. This suggests that the biosensor with the covalently immobilized LOx displayed a better stability at higher temperatures. A control experiment was done to determine the effect of the temperature on LOx in solution (non-immobilized) (**Fig. 5B**). The results reveal that the response of the protein after incubation at the different temperatures decreased after 50°C. In general, immobilization of LOx onto hydrophobic SWCNT negatively affected its thermostability, regardless of the method of immobilization.

In a similar experiment, each biosensor was incubated at 60°C for a different period of time (0-35 min) (**Fig. 5C**). Chronoamperometry experiments were used to determine the response of the biosensor after incubation. The response of both biosensors decreased after 35 min of incubation at 60°C. The biosensor with the covalently immobilized enzyme showed a higher response throughout the entire time range than the one with the adsorbed enzyme. The results support the idea that the covalent bond between the protein and the SWCNT stabilized the protein at higher temperatures compared to the adsorbed enzyme. The formation of covalent bonds between the enzyme and the SWCNT could reduce its conformational flexibility thus preventing unfolding and denaturation at high temperatures (Hanefeld et al. 2009).

3.6. Repeatability and Long-Term Stability of the Biosensor

In order to study the response and stability of the biosensor after constant use, repeatability experiments were performed. A consecutive test of the biosensor adding 0.18 mM of lactate

was done until no-response was detected. Repeatability of the biosensor prepared with the covalently immobilized protein was compared to the one with adsorbed protein at room temperature. The results (**Fig. 6A**) show that both biosensors did not show any loss of activity after 15 analyses. The response of the covalently attached protein decreased 50% after 45 consecutive test, while the response of the electrode with adsorbed protein decreased 50% after 30 consecutive tests. At the beginning of the experiment during the first measurements the adsorbed biosensor displayed a higher response than the covalent immobilized biosensor; however, after consecutive use the response decreased more than that of the covalent biosensor. This behavior might be attributable to protein leaching out of the biosensor after constant used (Kim et al. 2006). In addition, as already discussed, covalent attachment could improve protein stability by reducing its conformational mobility.

Additionally, the long-term stability of the lactate biosensor was determined by measuring the relative activity after storage at different temperatures (4°C and at 30°C). The biosensor was tested every 2 days for a period of 30 days, and then every week for up to 70 days of storage. **Figures 6B and 6C** show the long-term stability of the two electrodes after different temperatures and incubation times. When the electrodes were stored at 4°C (**Fig. 6B**), the response of the electrodes decreased for about 50 days and then reached a steady state with a low response. Even though both electrodes showed the same long-term stability at 4°C, the response of the covalent immobilized protein electrode was higher than that of the adsorbed protein electrode during the entire profile. After 25 days of storage at 4°C, the sensors with covalently and adsorbed enzyme show 40% and 20% of relative activity, respectively.

Table S1 presents a review of some parameters on the long-term stability of some LOx biosensors with the protein directly immobilized onto CNTs or entrapped in CNT-polymer matrixes. Our biosensor shows a comparable stability with the most stable biosensors in Table S1; however, many of them were tested only 4-6 times throughout the complete storage period while our biosensor was tested up to 20 times during the 70 d storage period.

Similar results were observed when both electrodes were incubated at 30°C (**Fig. 6B**). At this temperature both electrodes lost all activity in only 8 days, but the adsorbed protein showed a lower response compared to the covalent electrode during the experiment. Again, this result could be due to leaching of the adsorbed protein during constant use or protein stability differences. An analogous experiment done at 37°C incubation temperature showed no activity after only one-day of incubation.

4. Conclusions

This paper presents a comprehensive comparative study of two protein immobilization methods, i.e., physical adsorption and covalent immobilization, for the construction of a LOx biosensor. Herein, we demonstrate that when LOx is covalently immobilized onto a SWCNT electrode the response decreased compared with the biosensor with adsorbed protein. However, the thermostability and the long-term stability are improved compared to the biosensor with the adsorbed protein. A possible explanation could be reduced structural dynamics of the enzyme as the result of the covalent immobilization, which would cause

reduced enzyme activity and improved enzyme stability. Covalent enzyme immobilization also reduced protein leaching.

Other carbon-based materials (e.g., graphene, multi walled-CNT) should be explored in the future as well because they offer advantages in particular for the covalent enzyme immobilization since they offer more surface area and potential immobilization sites (e.g., carboxyl groups).

Supplementary Material

Refer to Web version on PubMed Central for supplementary material.

Acknowledgments

This publication was supported by the grant SC1 GM086240 from the National Institutes of Health (NIH) and by NASA URC Grant NNG05GG78H. MP received the fellowship Puerto Rico NASA Space Grant Consortium and the NASA Jenkins Pre-doctoral Fellowship Project (JPFP). The authors would like to thank Dr. Lenibel Santiago for some help in this work. We thank the Materials Characterization Center (MCC) and the NASA Center for Advanced Nanoscale Materials (NASA-CANM) at University of Puerto Rico for the use of the AFM and the XPS instruments.

REFERENCES

Asuri P, Karajanagi SS, Sellitto E, Kim DY, Kane RS, Dordick JS. Biotechnol. Bioeng. 2006; 95:804–811. [PubMed: 16933322]

Bakker J, Gris P, Coffernils M, Kahn RJ, Vincent JL. Am. J. Surg. 1996; 171:221–226. [PubMed: 8619454]

Boero C, Carrara S, Del Vecchio G, Calzá L, De Micheli G. Sens. Actuators B: Chem. 2011; 157:216–224.

Cang-Rong JT, Pastorin G. Nanotechnology. 2009; 20 Article 10.1088/0957-4484/20/25/25510.

Cowan BN, Burns HJG, Boyle P, Ledingham IM. Anaesthesia. 1984; 39:750–755. [PubMed: 6476309]

Flavel BS, Garrett DJ, Lehr J, Shapter JG, Downard AJ. Electrochim. Acta. 2010; 55:3995–4001.

Furuichi M, Suzuki N, Dhakshnamoorhty B, Minagawa H, Yamagishi R, Watanabe Y, Goto Y, Kaneko H, Yoshida Y, Yagi H, Waga I, Kumar PKR, Mizuno H. J. Mol. Biol. 2008; 378:436–446. [PubMed: 18367206]

Goran JM, Lyon JL, Stevenson KJ. Anal. Chem. 2011; 83:8123–8129. [PubMed: 21942440]

Gupta RK, Periyakaruppan A, Meyyappan M, Koehne JE. Biosens. Bioelectron. 2014; 59:112–119. [PubMed: 24709327]

Haghighi B, Bozorgzadeh S. Talanta. 2011; 85:2189–2193. [PubMed: 21872077]

Hanefeld U, Gardossi L, Magner E. Chem Soc Rev. 2009; 38:453–468. [PubMed: 19169460]

Huang J, Li J, Yang Y, Wang X, Wu B, Anzai J.-i. Osa T, Chen Q. Mater. Sci. Eng. C. 2008; 28:1070–1075.

Im JE, Han JA, Kim BK, Han JH, Park TS, Hwang S, Cho SI, Lee WY, Kim YR. Surf. Coat. Technol. 2010; 205:S275–S278.

Kim J, Jia HF, Wang P. Biotechnol. Adv. 2006; 24:296–308. [PubMed: 16403612]

Liu X, Neoh KG, Cen L, Kang ET. Biosens. Bioelectron. 2004; 19:823–834. [PubMed: 15128101]

Liu ZF, Shen ZY, Zhu T, Hou SF, Ying LZ, Shi ZJ, Gu ZN. Langmuir. 2000; 16:3569–3573.

Moore KE, Flavel BS, Shearer CJ, Ellis AV, Shapter JG. Electrochem. Commun. 2011; 13:1190–1193.

Nan XL, Gu ZN, Liu ZF, Pagán M, Solá R, Griebenow K. J. Colloid Interface Sci. Biotechnol. Bioeng. 2002; 2009; 245103(1):311–318. 77–84. [PubMed: 16290365]

Petrovykh DY, Kimura-Suda H, Opdahl A, Richter LJ, Tarlov MJ, Whitman LJ. Langmuir. 2006; 22:2578–2587. [PubMed: 16519457]

Rosario-Castro BI, Contes-de-Jesus EJ, Lebron-Colon M, Meador MA, Scibioh MA, Cabrera CR. Appl. Surf. Sci. 2010; 257:340–353.

Rosario-Castro BI, Fachini ER, Hernandez J, Perez-Davis ME, Cabrera CR. Langmuir. 2006; 22:6102–6108. [PubMed: 16800665]

Saifuddin N, Raziah AZ, Junizah AR. Journal of Chemistry. 20132013:18. Article 10.1155/2013/676815.

Sanchez-Pomales G, Cabrera CR. J. Electroanal. Chem. 2007; 606:47–54.

Sassolas A, Blum LJ, Leca-Bouvier BD. Biotechnol. Adv. 2012; 30:489–511. [PubMed: 21951558]

Solá RJ, Rodriguez J, Griebenow K. Cell. Mol. Life Sci. 2007; 64(16):2133–2152. [PubMed: 17558468]

Shapiro NI, Howell MD, Talmor D, Nathanson LA, Lisbon A, Wolfe RE, Weiss JW. Ann. Emergency Med. 2005; 45:524–528.

Stavyiannoudaki V, Vamvakaki V, Chaniotakis N. Anal. Bioanal. Chem. 2009; 395:429–435. [PubMed: 19644678]

Taurino I, Reiss R, Richter M, Fairhead M, Thony-Meyer L, De Micheli G, Carrara S. Electrochim. Acta. 2013; 93:72–79.

Vashist SK, Zheng D, Al-Rubeaan K, Luong JHT, Sheu F-S. Biotechnol. Adv. 2011; 29:169–188. [PubMed: 21034805]

Wang HJ, Yin GP, Shao YY, Wang ZB, Gao YZ. J. Power Sources. 2008; 176:128–131.

Wang T, Fu Y, Bu L, Qin C, Meng Y, Chen C, Ma M, Xie Q, Yao S. J. Phys. Chem. C. 2012; 116:20908–20917.

Weber J, Kumar A, Kumar A, Bhansali S. Sens. Actuators B: Chem. 2006; 117:308–313.

Yamamoto K, Shi G, Zhou T, Xu F, Xu J, Kato T, Jin JY, Jin L. Analyst. 2003; 128:249–254. [PubMed: 12705383]

Highlights

- We characterized and compared two differently constructed nanostructured lactate biosensors.
- The enzyme lactate oxidase was covalently deposited onto carbon nanotubes in one sensor and deposited by adsorption in the other.
- Functional and stability tests revealed better operational and storage stability in case of the biosensor employing the immobilized enzyme.

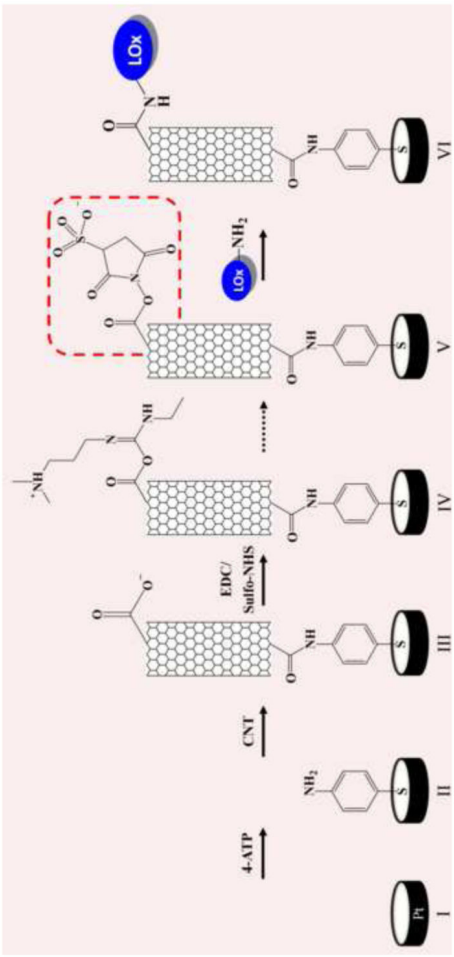

Figure 1.
Steps of the lactate oxidase biosensor construction.

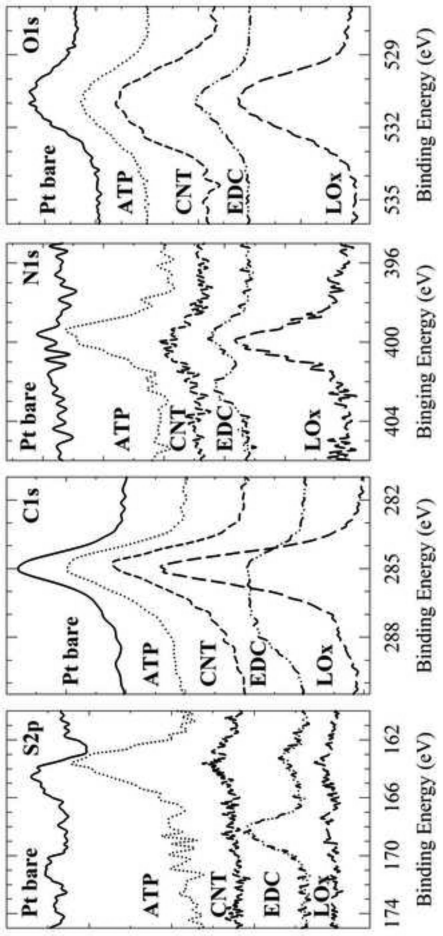

Figure 2.

XPS high resolution S2p, C1s, N1s, O1s spectra for each immobilization step of the biosensor assembly: bare Pt (solid line), 4-ATP (dotted line), SWCNT (small dashed line), SWCNT with EDC/Sulfo-NHS linker (dotted-dashed line), and LOx (large dashed line).

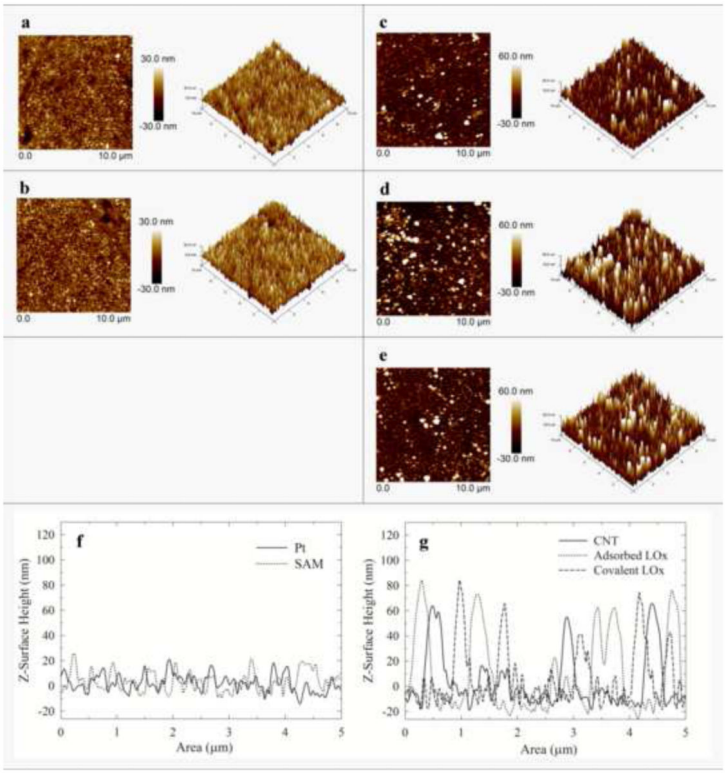

Figure 3.

AFM micrographs for each immobilization step of the biosensor assembly: (a) bare Pt, (b) 4-ATP (c) SWCNT (d) adsorbed LOx, and (e) covalently immobilized LOx. All images have a scan size of 10.0 μm. Right images are the 3D views of the images on the left. Cross section analysis of the AFM images: (f) bare Pt (solid line) and 4-ATP (dotted line); (g) CNT (solid line), adsorbed LOx (dotted line) and covalently immobilized LOx (dashed line).

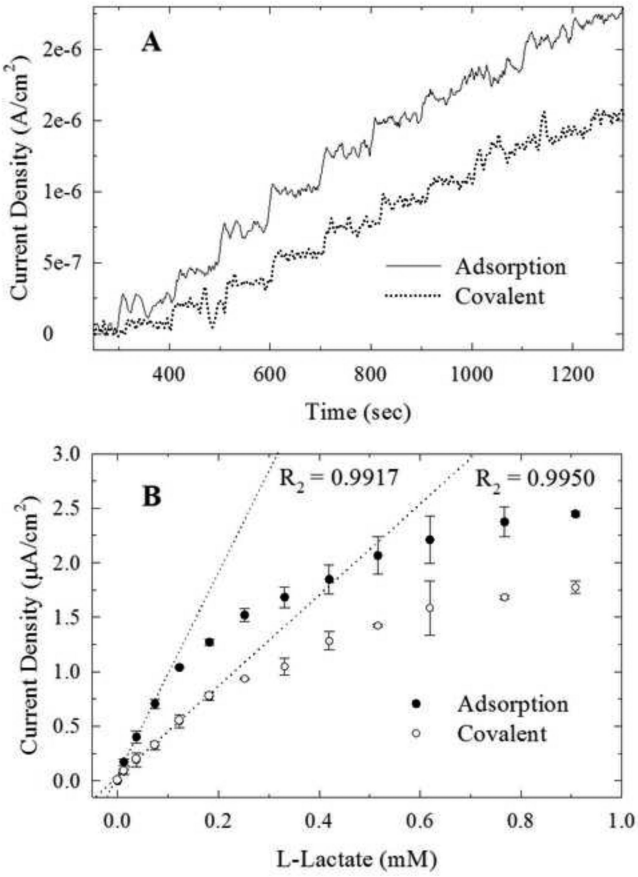

Figure 4.

Chronoamperometric response (A) and calibration curves (B) of the adsorbed (solid line; closed circles) and covalently immobilized (dotted line; open circles) LOx biosensor after successive additions of 6.0 mM L-lactate (E = 0.6 V).

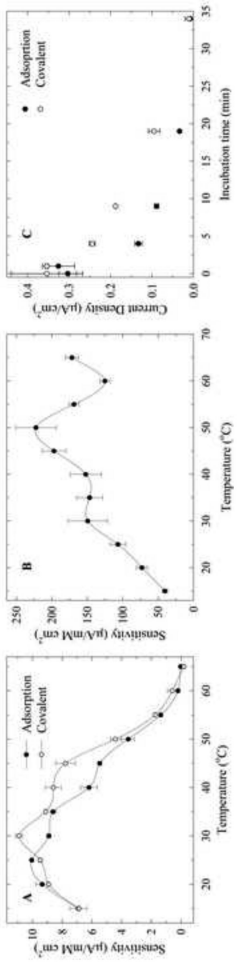

Figure 5.

Effect of temperature on the biosensor response after 15 min incubation for the adsorbed (closed circles) and covalently immobilized (open circles) LOx biosensor (A); and for LOx in solution using a SWCNT sensor (0.68 μM LOx) (B). Thermostability of the physically adsorbed (closed circles) and covalently immobilized (open circles) LOx biosensor after different incubation times at 60°C (C). (0.18 mM L-lactate; 0.6 V)

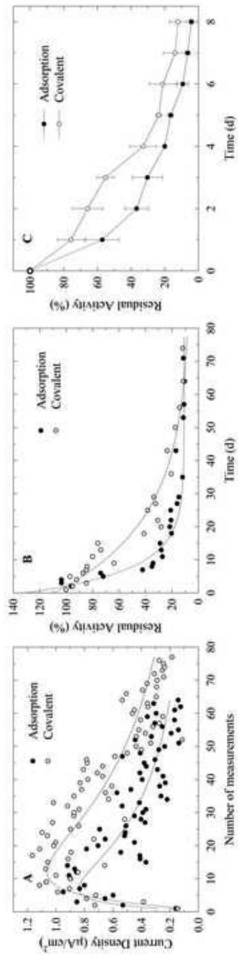

Figure 6.

Repeatability experiments after consecutive tests of the adsorbed (closed circles) and covalently immobilized (open circles) LOx biosensor (A). Long-term storage stability of the adsorbed (closed circles) and covalently immobilized (open circles) LOx biosensor after 72 d storage at 4°C (B) and 8 d storage at 30°C (C). (0.18 mM of lactate; 0.6 V)